An Automated Methodology for Fetal Heart Rate Extraction From the Abdominal Electrocardiogram

Evaggelos C. Karvounis, *Student Member, IEEE*, Markos G. Tsipouras, *Student Member, IEEE*, Dimitrios I. Fotiadis, *Senior Member, IEEE*, and Katerina K. Naka

***Abstract*—This paper introduces an automated methodology for the extraction of fetal heart rate from cutaneous potential abdominal electrocardiogram (abdECG) recordings. A three-stage methodology is proposed. Having the initial recording, which consists of a small number of abdECG leads in the first stage, the maternal R-peaks and fiducial points (QRS onset and offset) are detected using time–frequency (t–f) analysis and medical knowledge. Then, the maternal QRS complexes are eliminated. In the second stage, the positions of the candidate fetal R-peaks are located using complex wavelets and matching theory techniques. In the third stage, the fetal R-peaks, which overlap with the maternal QRS complexes (eliminated in the first stage) are found using two approaches: a heuristic algorithm technique and a histogram-based technique. The fetal R-peaks detected are used to calculate the fetal heart rate. The methodology is validated using a dataset of eight short and ten long-duration recordings, obtained between the 20th and the 41st week of gestation, and the obtained accuracy is 97.47%. The proposed methodology is advantageous, since it is based on the analysis of few abdominal leads in contrast to other proposed methods, which need a large number of leads.**

***Index Terms*—Abdominal electrocardiogram (abdECG), fetal electrocardiogram (fECG), fetal heart rate (fHR), time–frequency (t–f) analysis.**

I. Introduction

THE abdominal electrocardiogram (abdECG) is the recording of the cardiac activity of both the mother and the fetus. It is recorded by placing several leads on the abdomen (and sometimes the thorax) of the mother. The fetal electrocardiogram (fECG) can be derived from the abdECG and can be used for the extraction of fetal heart rate (fHR), which is a marker for the cardiac condition of the fetus [1].

The most common technique for recording fHR during pregnancy is the Doppler ultrasound. Although used throughout the world, such systems present several disadvantages. More specifically, they require intermittent repositioning of the transducer, and they are only suitable for use with highly trained midwifes. Also, the ultrasound transducer is cumbersome and uncomfortable while the procedure involves launching a 2-MHz signal towards the fetus. Therefore, it is considered as an invasive technique, and it is not recommended, especially, for long-time recordings. On the contrary, the abdECG offers several advantages over Doppler ultrasound; lightweight electrodes are used and it is simple to operate even by the mothers themselves, therefore, can be used in the normal home environment. The procedure is noninvasive and can be used for long-duration recordings [2].

The fECG exhibits a bandwidth of 0.05–100 Hz. In an abdominal register, the maximum amplitude of the QRS usually oscillates from 100–150 μV for the maternal recording, and up to 60 μV for the fetal recording. The energy of the latter has been estimated to be less than one quarter of the total signal energy [3], [4]. Moreover, the spectra of both signals overlap; it is consequently not possible to separate them using conventional frequency selective filtering. The main source of interference is the maternal electrical activity, the amplitude of which is much higher than the amplitude of the fetus electrical activity and is often completely masked by the former. The fECG signals are often obscured by electrical noise from other sources. Common ECG noise sources such as power line interference, muscle contractions, respiration, in addition to electromyogram (EMG), and electrohysterogram (EHG), due to uterine contractions, can corrupt fECG signals significantly [5]. Also, the shape of the fECG signal depends on the position of the electrodes (there is no standard electrode positioning for optimal fECG acquisition [6]), on the gestational age and the position of the fetus [7]. All of the aforementioned constraints make the fECG extraction a difficult process.

II. Related Work

Various research efforts have been carried out in the area of fECG and fHR extraction, including auto and cross correlation techniques [8], subtraction of an averaged pattern [9], matched filtering [2], linear regression [10], adaptive filtering [3], [11], [12], fractals [13], neural networks [4], [14], infinite impulse response (IIR) adaptive filtering combined with genetic algorithms [15], temporal structure [16], fuzzy logic [17], [18], frequency tracking [19], polynomial networks [20], signal's kurtosis analysis [21], and time domain analysis [22]. The wavelet transform is another approach that has been proposed for fECGs processing. Various techniques for noise removal and detection of fetal waveforms have been used, involving Gabor-8 wavelets

Manuscript received February 14, 2006; revised April 13, 2006. This work was supported in part by the program "HERAKLITOS" of the Operational Program for Education and Initial Vocational Training of the Hellenic Ministry of Education.

E. C. Karvounis is with the Department of Materials Science and Engineering, University of Ioannina, Ioannina GR 45110, Greece (e-mail: ekarvuni@cc.uoi.gr).

M. G. Tsipouras is with the Unit of Medical Technology and Intelligent Information Systems, Department of Computer Science, University of Ioannina, Ioannina GR 45110, Greece (e-mail: markos@cs.uoi.gr).

D. I. Fotiadis is with the Unit of Medical Technology and Intelligent Information Systems, Department of Computer Science, University of Ioannina, GR 45110, Ioannina, Greece, and also with the Biomedical Research Institute—Foundation of Research and Technology Hellas (FORTH), Ioannina GR 45110, Greece (e-mail: fotiadis@cs.uoi.gr).

K. K. Naka is with the Department of Cardiology, Medical School, University of Ioannina, Ioannina GR 45110, Greece, and also with the Michaelidion Cardiology Center, Ioannina GR 45110, Greece (e-mail: anaka@cc.uoi.gr).

Digital Object Identifier 10.1109/TITB.2006.888698

and Lipschitz exponent's theory [23], biorthogonal quadratic spline wavelet and modulus maxima theory [24] and complex continuous wavelets [25].

The extraction of fECG from the mixed signal (mother and fetus) can be reframed in a more efficient manner using blind source separation (BSS) methods [26]. BSS methods consist of extracting unknown signals (called sources), which are assumed to be statistically independent, from a few known mixtures of these signals. The main advantage of these techniques is that they do not require any *a priori* knowledge about the signals (contrary to filtering methods). The BSS methods are divided into two major groups, the one that use second-order statistics, performing principal component analysis (PCA) [5], [27], [28] or singular value decomposition [18], [28]–[30], and those that take advantage of the higher order statistical information contained in the available data, performing independent component analysis (ICA) [11], [28], [31], [32]. Some proposed ICA-based techniques are the INFOMAX [33], the JADE [34], the FastICA [35] and the MERMAID [36] algorithms. BSS in the wavelet domain [37], and an adaptation of the wavelet-ICA (WICA) method [38] have also been proposed. The main disadvantage of the BSS-based methods is that they require a large number of recorded ECG leads; the larger the number of the sources, the better the results of the analysis. Each electrode must record a different mixture of sources, and hence, the electrodes must be scattered on the mother's body, and further, thoracic electrodes are required [6]. Therefore, the use of these methods is limited in cases of nonclinical environment systems (i.e., homecare devices) where the recording of a large number of sources makes their application difficult and uncomfortable. Also, all BSS-based algorithms suffer from the problem of scale and permutation, i.e., the output channel corresponding to the signal of interest (fECG) is never known and must be determined by an expert.

III. Our Approach

In this paper, a three-stage methodology for the automated detection of fetal heart beats and the fHR extraction is presented. The methodology is based on the analysis of leads of the abdECG signal. In the first stage, the abdECG is analyzed using the smoothed pseudo Wigner–Ville distribution (SPWVD) [39]. The areas of high-energy concentration are detected, and they are used to identify the maternal R-peaks (mR-peaks) and the fiducial points (QRS onset and offset). The maternal fiducial points are used to eliminate the maternal QRS (mQRS) complexes from the abdECG. In the second stage, complex wavelets are used in order to detect the candidate fetal R-peaks (fR-peaks). False cases (artefacts) are included, but not fR-peaks that overlap with the mQRSs (eliminated in the previous stage). Acceptance or rejection of the candidate fR-peaks is materialized utilizing matching techniques, which are based on a set of fetal QRS complex (fQRS) patterns, which are introduced by medical experts. The detection of the overlapped fR-peaks is accomplished in the third stage. Two different approaches are employed: the first is based on a heuristic algorithm, which involves medical knowledge, while the second is a histogram-based technique. The detected fR-peaks are used to extract the fHR.

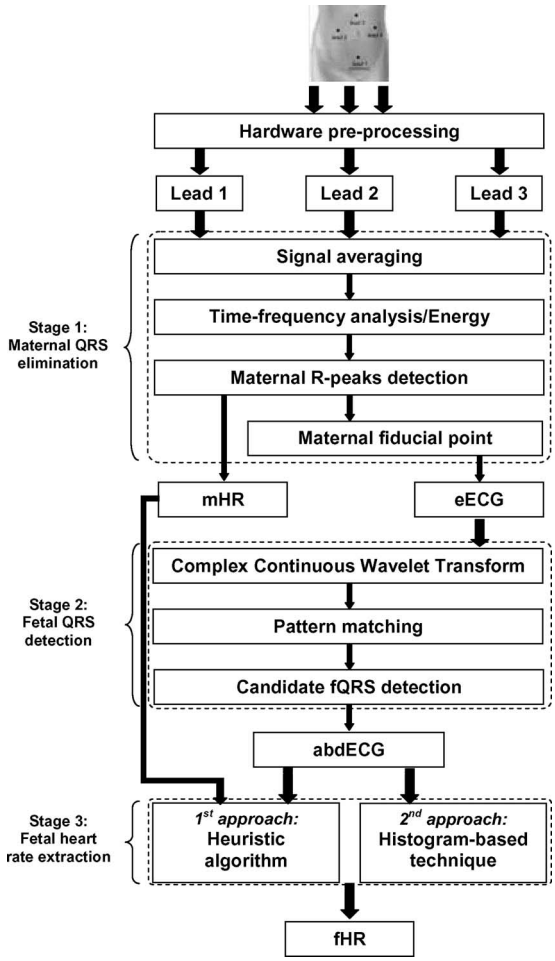

Fig. 1. Proposed three-stage methodology.

The proposed methodology is based on the analysis of the abdECG, in order to extract the fHR, and thus, exhibits the advantages of the abdECG recording over that of the Doppler ultrasound such as ease of operation, noninvasiveness, long-duration monitoring ability, and mobility. Also, the analysis is carried out using only three abdECG leads that can also be applied using just one or two leads. If these leads include substantial fECG information, then thoracic leads are not required. Also, the methodology employs time–frequency (t–f) analysis and wavelets to address the nonstationary behavior of the signal. The evaluation is made using a large number of real abdECG records, from several subjects, covering a large period of the gestation.

The remainder of the paper is structured as follows: initially, the three-stage methodology along with the dataset used to evaluate it are described in detail. Results of the evaluation of the proposed methodology are presented in Section V and the discussion is carried out in Section VI. Also, a comparison between the proposed methodology and other approaches is presented in the discussion section. Finally, the conclusions and several thoughts about future work are given in Section VII.

IV. Materials and Methods

The dataset used for our methodology along with the stages of the three-stage methodology, shown in Fig. 1, is described in detail below.

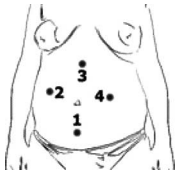

Fig. 2. Electrode placements.

A. Dataset

We use abdominal signals, which are obtained from a database created at the University of Nottingham [2]. Signals are acquired using four electrodes placed on the mother's abdomen (Fig. 2) by a low-noise, general-purpose electrophysiological recorder. The first electrode (electrode 1 in Fig. 2) is placed on the symphysis pubis and it is considered as common to the three input channels, while the other electrodes are placed, as shown in Fig. 2. Thus, three bipolar input channels (leads) are obtained. During the recording, the data were passed through a band-pass filter with high-frequency and low-frequency cutoffs at 100 and 4 Hz respectively, which is the bandwidth of interest for fECG monitoring.[1] The recordings are digitized using a 12-bit analog-to-digital converter. The sampling frequency is 300 Hz, and the highest gain of the unit (in its fECG configuration) is 7800. The measurements are simultaneously recorded from all three channels. The database consists of eight short recordings (60 s each), obtained from eight different women and ten long recordings (15 min each), obtained from five different women. The abdECG records are obtained between the twentieth and forty-first week of gestation.

B. Stage 1: mQRS elimination

This stage includes signal averaging, t–f analysis and energy calculation, mR-peaks detection, and maternal fiducial point detection. All the abdECG leads are utilized, and the outcome is the eECG signal (abdECG signal with the maternal QRSs eliminated) and the maternal heart rate (mHR).

1) Signal Averaging: The average of all available leads (three in our dataset) is calculated and the dc of the average signal is removed; the output is the abdECG signal

$$\text{abdECG}(t) = \sum_{i=1}^{M} \text{lead}_i(t) - \frac{1}{N} \sum_{t=1}^{N} \sum_{i=1}^{M} \text{lead}_i(t) \qquad (1)$$

where M is the number of the available leads, t is time instant, $\text{lead}_i(t)$ is the sample of the lead i at the time instant t, and N is the length (number of samples) of each lead.

2) t–f Analysis: The WVD [39]–[42] is a very powerful and appealing tool for the analysis of nonstationary, nonlinear, and transient signals, widely used in the field of t–f feature extraction. A windowed version of the WVD is the smoothed pseudo WVD (SPWVD), which is defined as

$$\text{SPWVD}_x(t,\omega) = \int_{-\infty}^{+\infty} h(s) \left(\int_{-\infty}^{+\infty} g(\tau)\, x\left(t+\frac{\tau}{2}\right) \times x^*\left(t-\frac{\tau}{2}\right) e^{-j2\pi\omega\tau}\, d\tau \right) ds \qquad (2)$$

where $x(\cdot)$ is the signal, t is the time, ω is the frequency, and $h(\cdot)$ and $g(\cdot)$ are window functions centered at time τ and frequency s, respectively. The SPWVD can substantially suppress the cross terms, but reduce the resolution. In the proposed methodology, the SPWVD is applied to the abdECG signal. Fig. 3(a) shows the abdECG signal, and Fig. 3(b) its power spectral density (PSD). The time window is a Hamming 64-point length window, while the frequency window is a Hamming 32-point long window. The PSD function is integrated with respect to frequency to extract the energy $E(t)$

$$E(t) = \left(\int_{-\infty}^{+\infty} \text{SPWVD}_x\,(t,\omega)\, d\omega \right)^2. \qquad (3)$$

The $E(t)$ of the abdECG is shown in Fig. 3(c).

3) Maternal R-Peak Detection: Using the $E(t)$ of the abdECG, the maternal R-peaks are detected as follows: for a time instant t_i, if $E(t_i) > \theta$, then, t_i is considered as a candidate mR-peak. The threshold θ is adaptive to each record, and is computed as $\theta = 10/N \sum_{t=1}^{N} E(t)$. Two medical rules are applied to include or reject a candidate mR-peak [43]. For two consecutive candidate mR-peaks located at t_i and t_j:

Rule 1) *If* $t_j - t_i < 0.2s$, *then* the candidate mR-peak corresponding to the minimum $E(\cdot)$ value is rejected (two R-peaks closer than 0.2 s cannot exist in the ECG).

Rule 2) *If* $t_j - t_i > 2s$, *then* the time instant corresponding to the maximum $E(\cdot)$ value between the candidate mR-peaks, is considered as a candidate mR-peak (a

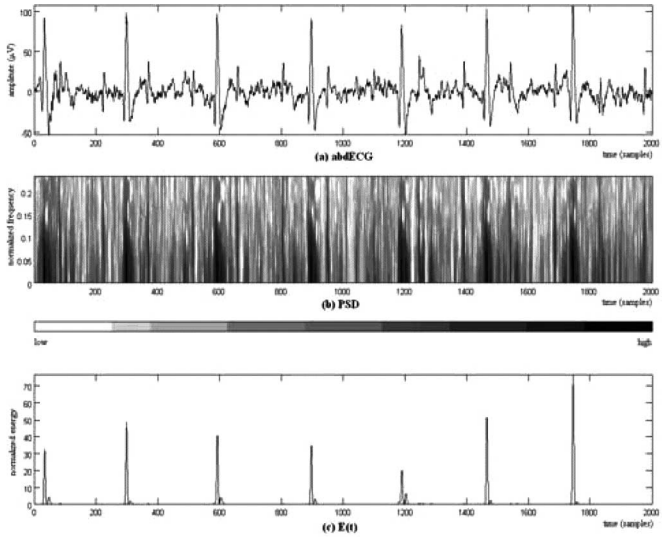

Fig. 3. Time–frequency analysis. (a) abdECG signal, (b) PSD of the abdECG signal, and (c) energy distribution versus time.

[1]In the literature, the suggested bandwidth is 0.05–100 Hz, but the above cutoff frequencies have been used in [2] since the authors found removal artefacts outside this region.

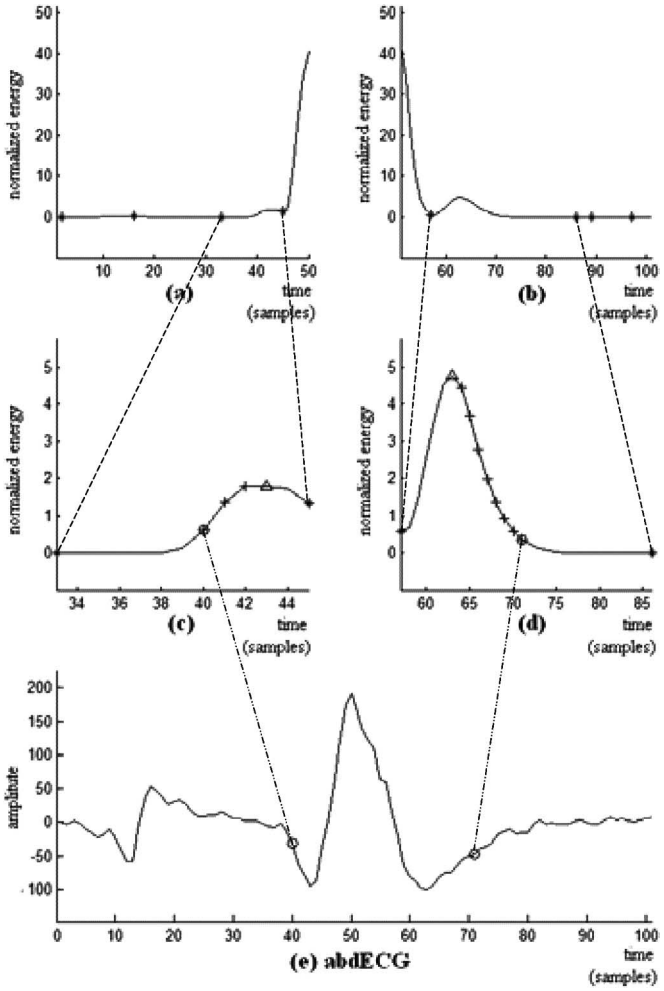

Fig. 4. Maternal fiducial point detection. (a) $E(t)$ for the sub-window $[t_i - 50,\ t_i)$ time interval and the local minima (noted with *stars*). (b) $E(t)$ for the sub-window $(t_i,\ t_i + 50]$ time interval and the local minima (noted with *stars*). (c) Search for the $t_{Q_i}^{\text{start}}$ (the *triangle* denotes the initial point, the *crosses* correspond to the search steps, while the *circle* with the cross denotes the final $t_{Q_i}^{\text{start}}$ point). (d) Search for the $t_{S_i}^{\text{end}}$ (the *triangle* denotes the initial point, the *crosses* correspond to the search steps, while the *circle* with the cross denotes the final $t_{S_i}^{\text{end}}$ point). (e) abdECG signal with the fiducial points (noted with *circles*).

time interval greater than 2 s does not exist in the ECG without an R-peak).

The above rules are applied recursively until no candidate mR-peak is rejected (from rule 1), and no new candidate mR-peak is included (from rule 2). From the remaining candidate mR-peaks the mHR is calculated.

4) Maternal Fiducial Point Detection: The maternal Q-wave start (mQRS onset) and S-wave end (mQRS offset) are detected using the $E(t)$ of the abdECG and the mR-peaks, as follows: a window of 101 samples is centerd at the ith mR-peak (t_i), and the subwindows, $[t_{i-50}, t_i]$ and $[t_i, t_{i-50}]$ are searched for the Q-wave start and the S-wave end, respectively. The local minima of $E(t)$ are found in both subwindows [Fig. 4(a) and (b)]. The first local minimum before the t_i point defines the end of the Q wave $(t_{Q_i}^{\text{end}})$, while the second local minimum before the t_i point (t_{Q_i}) defines the time interval $[t_{Q_i}, t_{Q_i}^{\text{end}}]$ [Fig. 4(c)], where the starting point of the Q wave $(t_{Q_i}^{\text{start}})$ is searched. The search procedure for the starting point of the Q wave $(t_{Q_i}^{\text{start}})$ is described below:

- initialization: $t = \underset{t\in[t_{Q_i}, t_{Q_i}^{\text{end}}]}{\arg\max}\ E(t)$;
- iteration: *while* $[[\int_t^{t_{Q_i}^{\text{end}}} E(t) < 0.99 \int_{t_{Q_i}}^{t_{Q_i}^{\text{end}}} E(t)]$ and $(t > t_{Q_i}]]$ then $t = t - 1$;
- $t_{Q_i}^{\text{start}} = t$.

The search is limited to the time interval

$$\left[t_{Q_i},\ \underset{t\in[t_{Q_i}, t_{Q_i}^{\text{end}}]}{\arg\max}\ E(t)\right].$$

The same procedure is followed for the identification of $t_{S_i}^{\text{start}}$ and $t_{S_i}^{\text{end}}$ points. The first local minimum after the t_i point is considered as the start of the S wave $(t_{S_i}^{\text{start}})$, while $t_{S_i}^{\text{end}}$ is searched within the $[t_{S_i}^{\text{start}}, t_{S_i}]$ time interval [Fig. 4(d)], where t_{S_i} is the second local minimum after the t_i point.

- initialization: $t = \underset{t\in[t_{S_i}^{\text{start}}, t_{S_i}]}{\arg\max}\ E(t)$;
- iteration: *while* $[[\int_{t_{S_i}^{\text{start}}}^{t} E(t) < 0.99 \int_{t_{S_i}^{\text{start}}}^{t_{S_i}} E(t)]$ and $(t < t_{S_i})]$ then $t = t + 1$;
- $t_{S_i}^{\text{end}} = t$.

The search is limited to the time interval

$$\left[\underset{t\in[t_{S_i}^{\text{start}}, t_{S_i}]}{\arg\max}\ E(t), t_{S_i}\right].$$

The $t_{Q_i}^{\text{start}}$ and $t_{S_i}^{\text{end}}$ points are the fiducial points of the ith mQRS complex [Fig. 4(e)].

After the maternal fiducial point detection, the mQRSs are eliminated from the abdECG signal: $\forall$mQRS$_i$, abdECG(t)=0, $\forall t \in [t_{Q_i}^{\text{start}}, t_{S_i}^{\text{end}}]$. Finally, the abdECG signal with the mQRSs eliminated (named eECG) is smoothed according to

$$\text{seECG}(t) = \text{eECG}(t) - \frac{1}{11}\sum_{k=-5}^{5} \text{eECG}(t+k) \qquad (4)$$

where seECG is the smoothed eECG. The initial abdECG, eECG, and seECG signals are shown in Fig. 5.

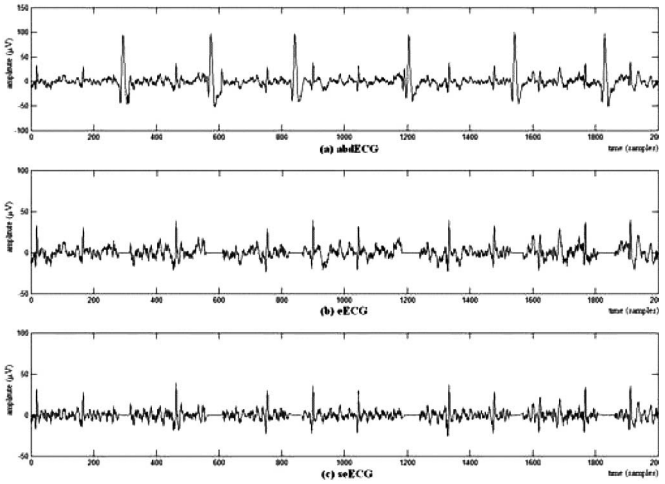

Fig. 5. Maternal QRS elimination and smoothing. (a) abdECG signal and the maternal fiducial points. (b) The signal after the maternal QRS elimination (eECG signal). (c) Smoothed eECG signal (seECG).

C. Stage 2: fQRS Detection

In this stage, initially, the seECG is analyzed using a complex continuous wavelet transform (CCWT), and next, the modulus of the coefficients is used to find the candidate fR-peaks using pattern matching. The outcome of this stage is the positions of the fR-peaks not overlapping with the mQRSs (eliminated in stage 1).

1) CCWT: It is used to decompose the signal into small oscillations that are highly localized in time. The result is a set of wavelet coefficients, whose magnitude indicates the similarity between the signal and the basic wavelets at various scales and locations. The CCWT [44]–[47] performs continuous wavelet analysis of real signals using complex wavelets. The complex nature of these wavelets provides further improvement in signal processing, compared to real-valued wavelet analysis [47]. CCWT can be used for the detection of waves represented by local maxima and minima of the signal, and for the identification of symmetric and antisymmetric waves. Using the square modulus of the CCWT, the maxima, minima, or even inflection points can be found.

In our methodology, the complex frequency B-spline wavelet [48] was used, due to its good temporal localization properties. The complex frequency B-spline wavelet is defined as

$$\psi(x) = \sqrt{f_b}\left(\sin c\left(\frac{f_b x}{m}\right)\right)^m e^{2\pi i f_c x} \tag{5}$$

where m is an integer order parameter, f_b is a bandwidth parameter, and f_c is the center frequency of the wavelet. A first-order wavelet $(m = 1)$ is used to reduce the computational complexity. We have selected $f_b = 1$ and $f_c = 0.5$. The fR-peak detection is accomplished using the modulus of the CCWT coefficients. The transitions in the seECG signal correspond to local maxima at different scales in the decomposition modulus. The frequency content of the seECG characteristic waves is different, so they are distinguished at different decomposition scales [47]. The energy of the fR-peak is the highest at the first scale, so the wavelet decomposition of the signal with the frequency B-spline wavelet is computed for this scale. The modulus of the wavelet-transformed signal (mCCWT) is accumulated and moving average is applied

$$\text{smCCWT}(i) = \frac{1}{11}\sum_{k=-5}^{5} \text{mCCWT}(i+k). \tag{6}$$

The smoothed mCCWT (smCCWT) signal is searched for local maxima using peak detection. When a local peak exceeds the adaptive threshold, it is stored as a fR-peak candidate. For each peak, a window of 0.3 s is centerd on it, and if there is a higher peak in this window, then the initial peak is rejected. After this process, the remaining peaks are considered as candidate fR-peaks. Fig. 6 illustrates the seECG, mCCWT, and smCCWT signals and the detected fR-peaks.

2) Pattern Matching: The candidate fR-peaks, which were detected above, are validated using a pattern-matching technique. For this purpose, four fQRS patterns were identified as follows: a subset of our database was studied and several candidate fQRS patterns were identified. Then, expert cardiologists selected four patterns that would cover most of the potential QRS morphologies observed. The fQRS patterns (pfQRS) are shown in Fig. 7. A 20-point length window is centered on each candidate fR-peak, and the seECG signal in this window is obtained, which is considered as fQRS: $\text{fQRS}_i(l) = \text{seECG}(t), l = 1, \ldots, 20,\ t = t_i - 10, \ldots, t_i + 9$, where t_i is the time instant of the ith candidate fR-peak and $i = 1, \ldots, K$, where K being the number of the candidate fR-peaks. Also, for each window i, the magnitude is obtained as $\text{mgn}_i = \max_l(\text{fQRS}_i(l)) - \min_i = \min_l(\text{fQRS}_i(l))$. The average magnitude (mean_mgn) for all windows is also calculated. Each candidate fR-peak is evaluated using a simple rule: if the normalized cross correlation between the fQRS_i and one of the pfQRS is higher than 0.6, and the mgn_i is greater than 60% and less than 200% of the mean_mgn, then the candidate fR-peak is accepted, else it is rejected. The 60% and 200% values were

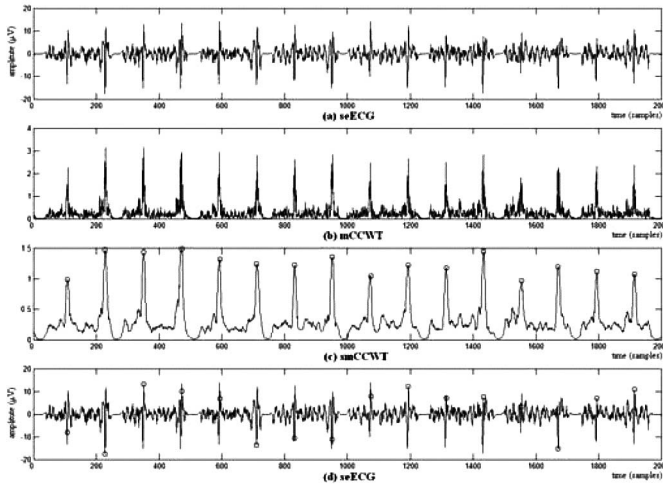

Fig. 6. Wavelet analysis and candidate fetal R-peak detection. (a) seECG signal, (b) modulus of the CCWT coefficients (mCCWT), (c) smoothed modulus of CCWT coefficients (smCCWT) and detected peaks (*circles*), and (d) seECG signal and candidate fetal R-peaks (*circles*).

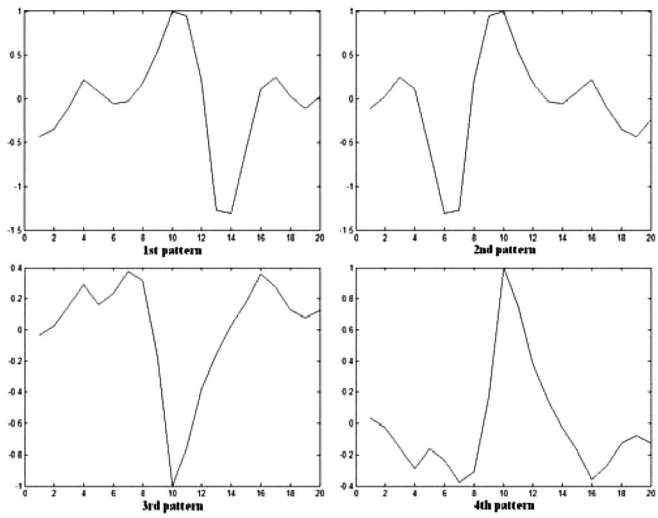

Fig. 7. Four fetal QRS patterns (pfQRS).

obtained heuristically. The procedure for the validation/rejection of the candidate fR-peaks, is summarized below.

if $(\max_{j=1,\ldots,4}(C(\text{fQRS}_i, \text{pfQRS}_j)) > 0.6)$
and $(\frac{\text{mgn}_i}{\text{mean\_mgn}} \in [0.6,\ 2])$
then the candidate fR-peak is accepted
else the candidate fR-peak is rejected.

The normalized cross correlation defined as $C(x,y) = \langle xy\rangle / \sqrt{\langle xx\rangle \langle yy\rangle}$, is a measure, timing the movements and proximity of alignment between two time series ($x(t)$ and $y(t)$). The length of the window is chosen to be 20 points (i.e., approximately 66 ms at 300-Hz sampling rate) due to the fact that the fQRS maximum length changes with respect to the week of gestation; the records included in this study were acquired up to the 34th week of gestation, for which the maximum fQRS length is approximately 65 ms [7].

D. Stage 3: fHR Extraction

In this stage, the fR-peaks that overlap with the mQRSs are found. For this purpose, two different approaches are tested: a heuristic algorithm, which involves medical knowledge, and a histogram-based technique. The heuristic algorithm utilizes the mR-peaks, detected in stage 1, and the fR-peaks, detected in stage 2, while the histogram-based technique utilizes only the fR-peaks. The results from each approach (fR-peaks overlapping with the mQRSs), combined with the fR-peaks detected from stage 2 are used to calculate the fHR.

1) Heuristic Algorithm: The heuristic algorithm utilizes the maternal and fR-peaks. Initially, the fetal RR interval signal (fRR) is extracted from the fR-peaks. Then, the median value of the fRR signal is calculated (fRR_m). Each fetal RR interval (fRR_i) is compared to the fRR_m. If $\text{fRR}_i > 1.5\ \text{fRR}_m$ then a possible overlapped fR-peak exists. To verify its existence, a window of 150 ms is centered on the center of the fRR_i interval, and if a mR-peak exists in this window, then, the mR-peak is considered as an overlapped fR-peak.

2) Histogram-Based Technique: In the second approach, the fR-peaks detected from stage 2 are used to compute the fRR interval signal and extract the histogram [Fig. 8(a)]. In the histogram, the time corresponding to the first peak [noted with the first circle in Fig. 8(a)] is considered as the "basic" fRR interval length (t_{RR}). Then, the $2t_{RR}$ is calculated [noted in Fig. 8(a) with the second circle]. All fRR intervals with length $t \in [2t_{RR} - \frac{t_{RR}}{2}, 2t_{RR} + \frac{t_{RR}}{2}]$ are considered as "double" fRR intervals, i.e., fRR intervals, which include one lost fR-peak, while all fRR intervals with length $t > 2t_{RR} + \frac{t_{RR}}{2}$ are considered as "multi" fRR intervals, i.e., fRR intervals that include two or more lost fR-peaks. The "double" fRR intervals are split in two fRR intervals, considering a fR-peak in the center of the "double" fRR interval. The "multi" fRR intervals are considered as highly "noisy" areas of the abdECG signal and no correction process is performed. As an example of this procedure, Fig. 8(b) shows part of a sample abdECG recording along with the detected fQRSs (noted with circles), and Fig. 8(a) shows the histogram [i.e., the number of fRR intervals found versus the fRR interval length, as they are indicated using circles for the detected fQRS in Fig. 8(b)], of the total abdECG recording.

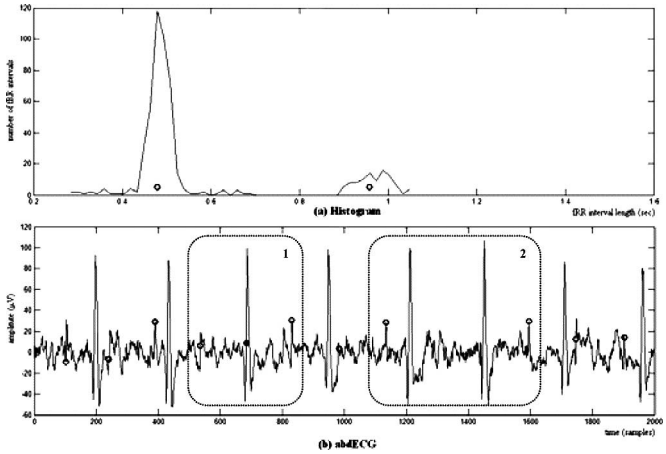

Fig. 8. Example of the histogram-based technique. (a) Histogram of the fRR interval signal. (b) "Double" fRR interval (marked by region 1) and "multi" fRR interval (marked by region 2). Fetal R-peaks are denoted with *circles* while the overlapped fetal R-peak that is detected from the histogram-based technique is denoted with the *black circle*.

V. Results

The proposed methodology is tested on the previously described dataset. The results for fR-peak detection are evaluated by an expert cardiologist, who calculated three quantitative results: true positive (TP) when a fR-peak is correctly detected by the proposed method, false negative (FN) when a fR-peak was not detected, and false positive (FP) when an artefact is detected as fR-peak. Indices of test performance can be derived from these results such as sensitivity, which is defined as $\text{Se} = \text{TP}/(\text{TP} + \text{FN})$, positive diagnostic value, which is defined as $\text{PDV} = \text{TP}/(\text{TP} + \text{FP})$, and accuracy, which is defined as $\text{Acc} = \text{TP}/(\text{TP} + \text{FP} + \text{FN})$. The Se defines the probability that a fR-peak is detected, while the PDV provides the probability that a detected fR-peak is actually a fR-peak and not a false detected artefact. Acc is a metric summarizing the positive and negative diagnostic values of a test or method [1].

Tables I and II present the results obtained from the evaluation of the proposed methodology for both the heuristic algorithm and histogram-based technique using the eight short-duration and the ten long-duration recordings, respectively. When the heuristic algorithm is used, the average Se is 95.49% for the short-duration recordings and 96.86% for the long-duration recordings. The average PDV is 99.80% for the short-duration recordings and 98.91% for the long-duration recordings, while the average Acc is 95.33% for the short-duration recordings and 95.84% for long-duration recordings, respectively. When the histogram-based technique is employed, the average Se is 99.37% for the short-duration recordings and 98.39% for the long-duration recordings and the average PDV is 99.82% for the short-duration recordings and 98.93% for the long-duration recordings. In this case, the average Acc is 99.19% for short-duration recordings and 97.35% for long-duration recordings, respectively. The short-duration recordings include a total of 1081 fR-peaks from which 49 were not detected (4.53%) when the heuristic algorithm is used, and seven were not detected (0.64%) when the histogram-based technique is used, while in

TABLE I
EVALUATION RESULTS USING THE EIGHT SHORT-DURATION RECORDS

		Heuristic algorithm						Histogram-based technique					
Recordings	**Duration**	**TP**	**FP**	**FN**	**Se(%)**	**PDV(%)**	**Acc(%)**	**TP**	**FP**	**FN**	**Se(%)**	**PDV(%)**	**Acc(%)**
Week 24	1 min	137	0	5	96.48	100	96.48	142	0	0	100	100	100
Week 26	1 min	129	0	6	95.55	100	95.56	135	0	0	100	100	100
Week 29	1 min	137	0	1	99.27	100	99.28	138	0	0	100	100	100
Week 35	1 min	128	0	1	99.22	100	99.22	129	0	0	100	100	100
Week 37	1 min	124	1	13	90.51	99.20	89.86	134	1	3	97.81	99.26	97.10
Week 39	1 min	135	1	10	93.10	99.26	92.47	144	1	1	99.31	99.31	98.63
Week 40	1 min	130	0	7	94.89	100	94.89	134	0	3	97.81	100	97.81
Week 41	1 min	112	0	6	94.91	100	94.92	118	0	0	100	100	100
TOTAL	**8 min**	**1032**	**2**	**49**	**95.49**	**99.80**	**95.33**	**1074**	**2**	**7**	**99.37**	**99.82**	**99.19**

TABLE II
EVALUATION RESULTS USING THE TEN LONG-DURATION RECORDS

		Heuristic algorithm						Histogram-based technique					
Recordings	**Duration**	**TP**	**FP**	**FN**	**Se(%)**	**PDV(%)**	**Acc(%)**	**TP**	**FP**	**FN**	**Se(%)**	**PDV(%)**	**Acc(%)**
w_HK_24	15 min	1913	6	77	96.13	99.69	95.84	1938	1	52	97.39	99.95	97.34
w_HK_28	15 min	1903	5	22	98.86	99.74	98.60	1915	0	10	99.48	100	99.48
w_HK_34	15 min	1580	99	61	96.28	94.10	90.80	1624	107	17	98.96	93.82	92.91
w_LD_20[1]	10 min	1254	4	19	98.51	99.68	98.20	1262	3	11	99.14	99.76	98.90
w_TA_20	15 min	1967	11	27	98.65	99.44	98.10	1987	4	7	99.65	99.80	99.45
w_WM_20	15 min	3055	10	55	98.23	99.67	97.92	3059	11	51	98.36	99.64	98.01
w_WM_24	15 min	1908	10	109	94.60	99.48	94.13	1935	10	82	95.93	99.49	95.46
w_MJ_20	15 min	2050	12	102	95.26	99.42	94.73	2094	15	58	97.30	99.29	96.63
w_MJ_24	15 min	2111	14	66	96.97	99.34	96.35	2162	14	15	99.31	99.36	98.68
w_LD_32	15 min	1730	26	89	95.11	98.52	93.77	1789	33	30	98.35	98.19	96.60
TOTAL	**145 min**	**19471**	**197**	**627**	**96.86**	**98.91**	**95.84**	**19765**	**198**	**333**	**98.39**	**98.93**	**97.35**

[1] The last five minutes are excluded from the study due to the fact that the fetal R-peaks cannot be identified by the medical expert and, therefore, results in the terms of TP, FN and FP cannot be obtained.

both cases, two artefacts (0.18%) are detected as fR-peaks. The long-duration recordings include a total of 20 098 fR-peaks from which 627 were not detected (3.12%) when the heuristic algorithm is used and 333 were not detected (1.66%) when the histogram-based technique is used, while 197 (0.98%) and 198 (0.99%) artefacts are detected as fR-peaks, when the heuristic algorithm and the histogram-based technique are used, respectively. The accuracy for both the short- and long-duration recordings is 97.47%. The Acc of the proposed methodology with respect to the week of the gestation is shown in Fig. 9.

Evaluation was also made using different lead combinations, i.e., applying the proposed methodology to only one lead and combinations of two leads. Table III presents the accuracy of the proposed methodology when it is applied to only the first, second, or third lead and combinations among them (first and second, second and third, third and first). The histogram-based approach is used for the detection of the fR-peaks that overlap with the mQRSs. Also, the respective results from Table II are included.

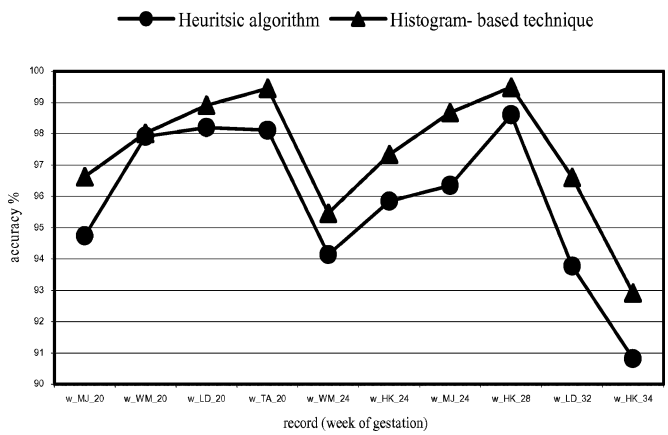

Fig. 9. Accuracy of the proposed method with respect to the week of gestation.

VI. DISCUSSION

The proposed methodology extracts the fHR from the abdECG signal. The methodology is designed such that it can be

TABLE III
ACCURACY (%) OF THE PROPOSED METHOD, USING SINGLE LEADS AND LEAD COMBINATIONS

	Single leads			Lead combinations			
Recordings	**1st**	**2nd**	**3rd**	**1st& 2nd**	**2nd&3rd**	**3rd&1st**	**all**
w_HK_24	94.94	95.24	99.80	95.95	97.06	97.50	97.34
w_HK_28	98.08	99.17	99.64	99.33	99.64	99.32	99.48
w_HK_34	93.23	94.67	39.56	95.81	82.90	90.93	92.91
w_LD_20	32.57	98.73	78.42	76.46	90.19	83.92	98.90
w_TA_20	99.15	98.86	43.07	99.60	94.82	99.45	99.45
w_WM_20	11.04	99.25	11.82	98.77	97.83	15.80	98.01
w_WM_24	74.88	90.57	46.74	86.61	87.53	90.41	95.46
w_MJ_20	63.71	76.83	79.20	79.34	76.88	89.87	96.63
w_MJ_24	97.08	91.28	95.82	97.25	96.24	84.08	98.68
w_LD_32	64.59	94.41	46.20	96.04	93.01	84.66	96.60

used when the number of the available abdECG leads is limited such as when wearable devices are employed. The nonstationary nature of the signal is handled using $t-f$ analysis and wavelets. Also, medical knowledge describing the fQRS shape patterns is employed in order to improve the efficiency of the proposed methodology.

Table III presents the accuracy of the methodology when it is applied to a single lead, a pair of leads and all three leads. As far as the single leads are concerned, most of the time, the results are very high using only the second lead; this is an expected result due to the position of the recording electrode used in the second lead (electrode 3), as shown in Fig. 2 which is in the middle axis of the abdomen and thus it is expected to carry fECG interference. Using only the first or the third lead might conclude to high, mediocre or poor results. This is also expected due to the position of the electrodes used for these leads (Fig. 2), which record the right and left axis of the abdomen, and thus, might not carry strong fECG interference. However, in some leads, for a certain time period, the fECG may be suppressed due to the movement of the fetus, etc. [2]. Concerning the lead combinations, the results in most of the cases, are comparable to the results of the single leads that are combined. A very interesting result is obtained when the combination of the third and first lead of the w_WM_24 record are used; the result is 74.88%, when only the first lead is used, and 46.74% when only the third lead is used, while their combination results to 90.41% accuracy (and 95.45% when all three leads are combined). This is probably due to the fact that the fECG interference is time-located to the first and the third lead. Similar behavior is observed in records w_LD_20, w_MJ_20, and w_LD_32. In all three leads, in some cases a single lead selection would improve the accuracy. All the above prove that our methodology can be implemented using just a single lead, if this lead carries strong fECG interference.

There are several methods proposed in the literature that employ BSS methods (PCA, SVD, and ICA) [5], [11], [27]–[36] for the fECG extraction. All BSS-based methods require a large number of recorded ECG leads in order to obtain satisfactory results, and suffer from the problem of scale and permutation. Most of the proposed methods are evaluated using simulated signals [4], [14]–[16], [18], [19], [21], [24], [28], [31], [32], [35], [37], or/and a very small dataset of real recordings [3]–[5], [11], [14], [16], [18], [20]– [24], [27]–[29], [34]–[36], [38]. The results presented are only qualitative [4], [5], [11]–[16], [18]–[21], [23], [27]–[29], [31], [34]–[36], [38]; no quantitative criterion that measures the quality of the signal of interest exists. Also, most of the time, both abdominal and thoracic leads are used [3]–[5], [11], [15], [16], [20], [21], and [27]–[29]. Extracting all the source signals from a large number of sensors, which may output hundreds of recordings, could take a long time. Thus, it is important to be able to extract only the desired signals instead of all sources. For this purpose, algorithms should be developed taking advantage of *a priori* medical knowledge.

TABLE IV
COMPARISON WITH EXISTING METHODS FOR FHR EXTRACTION

Author	**Description**	**Dataset**	**Accuracy (%)**
Pieri *et al.*, 2001 [2]	Matched filter	400 records (3 abdominal leads) Duration: 5-10 min	65
Mooney *et al.*, 1995 [12]	Adaptive algorithm	Several records (5 abdominal leads)	100
Azad, 2000 [17]	Fuzzy approach	5 records: (3 abdominal leads)	89[1]
Ibrahimy *et al.*, 2003 [22]	Statistical analysis	5 records: (1 abdominal lead) Duration: 20 min	89[2]
Karvounis *et al.*, 2004 [25]	Complex wavelets	15 records: (3 abdominal leads) Duration: 1 min	98.94
Current Work	Time-frequency analysis	8 short records (3 abdominal leads) Duration: 1 min	99.19
		10 long records (3 abdominal leads) Duration: 15 min	97.35

[1]Defined as $performance = \frac{TP-(FP+FN)}{TP}100\%$.

[2]Correlation coefficient between the simultaneous fHR measured from Doppler ultrasound and the method.

Table IV presents several methods proposed in the literature for the extraction of the fHR. All the methods were validated using real recordings (no simulated signals were involved), while all leads are placed on the abdomen of the mother (no thoracic leads were used). Due to the fact that there is no benchmark database for this area, and therefore, each approach is evaluated using different datasets, a direct comparison between the proposed methods is not feasible. The proposed methodology provides comparable results with the other methods. The method proposed by Mooney *et al.* [12] is not automated; areas of the abdECG are initially selected from a user, and then, the fHR

is calculated. Also, five to eight leads were used for the analysis, and when only the single channel with the highest signal to noise ratio was independently evaluated for each subject, the result was approximately 85%. The fuzzy-based approach by Azad [17] performed very well with 89% average performance (defined as performance$(\%) = 100(\mathrm{TP} - \mathrm{FP} - \mathrm{FN})/\mathrm{TP}$), but there is no reference about the exact number and duration of abdECG records used for the evaluation. Using the performance definition, the results of the proposed methodology are 95% for the short-duration recordings and 95.77% for the long-duration recordings, when the heuristic algorithm was used, and 99.16% for the short-duration recordings and 97.31% for the long-duration recordings, when the histogram-based technique is employed. Pieri *et al.* [2] use the larger dataset among all the methods presented in Table IV (400 records of 5–10 min each), but the results are rather poor (65%). The study by Ibrahimy *et al.* [22] also performs very well, and it is validated using a large dataset (five records of 20 min each), but the reported result (89%) is the correlation coefficient between the simultaneous fHR measured from Doppler ultrasound and the proposed method.

The proposed methodology is based on the analysis of abdECG leads; thoracic leads are not necessary. Also, the number of the initial sources (abdECG leads) is not important; the analysis can be carried out with a combination of two abdECG leads or even with a single abdECG lead, if it carries substantial fECG information (as previously discussed). Both these features are major advantages of the proposed methodology due to the fact that the placement of a large number of electrodes on the mother is difficult and impossible to be performed under nonclinical or mobile settings. Short-term monitoring of fHR, using Doppler ultrasound, has traditionally been used as a crude index of fetal health during pregnancy, and especially, during the last weeks of gestation, combined with monitoring of uterine contractions as part of cardiotocography. In case of high-risk pregnancies, more frequent or even long-term monitoring of fHR would be of great clinical value. However, this cannot be easily achieved or widely applied using Doppler ultrasound due to limitations inherent with its application, i.e., need for experienced personnel, specialized equipment, and use in hospital environments. Our methodology exhibits the advantages of the abdECG recording over the Doppler ultrasound (user-friendly, noninvasive, allows mobility, and long-duration monitoring), and thus, could be embedded in homecare devices or wearable systems. These, would be valuable for short- or long-term monitoring of fHR, especially, in high-risk pregnancies either at home or in hospital.

In the pattern-matching step of our methodology, we used four fQRS patterns in order to validate or reject candidate fQRS complexes. Four crude fQRS patterns were selected in order to be able to cover most of the QRS morphologies observed; a limited number of fQRS patterns was desirable such that laborious and time-consuming calculations could be minimized. This number is quite small compared to the large number of distinct fQRS morphologies that can be encountered. However, the method used subsequently to assess the similarity between the fQRS pattern and the fQRS candidate (cross correlation with a relatively low threshold of 0.6) has tolerance for small variations. This, combined with the crudeness of the selected fQRS patterns, means that small differences between the fQRS pattern and the fQRS candidate (such as positive or negative deflections at the beginning or end of the candidate fQRS complex, which, if taken into consideration, would induce a change in the fQRS morphology) would not affect the pattern matching. We can also understand that the use of the pattern selection is successful when one or two leads are used (Table III).

Our methodology automatically extracts the fHR from the abdECG leads, in contrast to BSS-based methods, which result in a set of signals, and a medical expert must define the signal of interest (fECG) to be further processed. Another advantage of our analysis is that it is validated with a large dataset comprised from real abdECG records and quantitative results are available. A disadvantage of the proposed methodology compared to the BSS based methods is that only the fHR signal is extracted (and the morphology of the fQRSs is also available although it is not used in this study) and not the entire fECG signal. Another limitation of the proposed methodology is the use of several parameters (i.e., the size of the smoothing windows, the 99% at the maternal fiducial point detection procedure), which are defined after extensive testing, along with the selection of the four fQRS patterns; both these features introduce a bias in the proposed methodology. Finally, there is no noise handling procedure in the proposed methodology; the electromyographic contamination, the power line interference, and the baseline oscillation are handled by the recording device.

VII. Conclusion

A methodology for the automated extraction of fHR from the abdECG signal has been developed. The methodology is based on t–f analysis and CCWT. Additionally, a heuristic algorithm and histogram-based technique are used to detect areas where the fQSRs overlap with mQRSs. Real abdECG records from several subjects, and covering almost all of the gestation period (from the 20th to 41st week) are incorporated for the validation of the methodology and the presented results indicate very high efficiency, since an overall accuracy of 97.47% is achieved. Both t–f analysis and CCWT are methodologies that have not been used before for fHR extraction. In the proposed method, the maternal and the fetal cardiovascular activity are treated as independent processes; no attempt has been made to further process the mQRSs or the mHR to extract information. This is mainly due to the fact that all recordings in our dataset are normal regarding the mECG. Therefore, there can be no significant information extracted from the mECG (such as significant rhythm variations or arrhythmic behavior). The selection of the fQRS patterns is another important issue; a wider selection of fQRS patterns instead of the small "crude" set used in this research might be a more accurate approach. Both these aspects, the exploitation of the relevance between the maternal and the fetal cardiovascular activity and the accurate definition of a large fQRS pattern database are very interesting subjects, and they will be addressed in future communications.

The major drawback of the proposed method is the difficulty to extract the fR-peaks in noisy background or in cases where the fECG is not easily distinguishable. The proposed fHR detection

method can be further improved, in terms of noise handling. The presence of noise in long-duration abdECG recordings is unavoidable, and proper filtering (either hardware or software) must be utilized. Also, further validation is needed with larger datasets and under real clinical or homecare conditions, in order to fully exploit the potential of the proposed methodology.

REFERENCES

[1] E. M. Symond, D. Sahota, and A. Chang, *Fetal Electrocardiography*. London, U.K.: Imperial College Press, 2001.

[2] J. F. Pieri, J. A. Crowe, B. R. Hayes-Gill, C. J. Spencer, K. Bhogal, and D. K. James, "Compact long-term recorder for the transabdominal foetal and maternal electrocardiogram," *Med. Biol. Eng. Comput.*, vol. 39, pp. 118–125, 2001.

[3] M. Martinez, E. Soria, J. Calpe, J. F. Guerrero, and J. R. Magdalena, "Application of the adaptive impulse correlated filter for recovering fetal electrocardiogram," in *Proc. Comput. Cardiol.*, Lund, Sweden, 1997, pp. 9–12.

[4] G. Camps Valls, M. Martinez Sober, E. Soria Olivas, R. Magdalena-Benedito, J. Calpe-Maravilla, and J. Guerrero-Martinez, "Foetal ECG recovery using dynamic neural networks," *Artif. Intell. Med.*, vol. 31, pp. 197–209, 2004.

[5] V. Zarzoso, A. K. Nandi, and E. Bacharakis, "Maternal and foetal ECG separation using blind source separation methods," *IMA J. Math. Appl. Med. Biol.*, vol. 14, pp. 207–225, 1997.

[6] V. Vrins, C. Jutten, and M. Verleysen, "Sensor array and electrode selection for non-invasive fetal electrocardiogram extraction by independent component analysis," in *Proc. 5th Int. Conf., ICA 2004*, Granada, Spain, Sep. 22–24, 2004, pp. 1017–1024.

[7] E. G. M. Golbach, J. G. Stinstra, P. Grot, and M. J. Peters, "Reference values for fetal MCG/ECG recordings in uncomplicated pregnancies," in *Proc. 12th Int. Conf. Biomagn.*, Espoo, Finland, 2000, pp. 595–598.

[8] S. Abboud, A. Alaluf, S. Einav, and D. Sadeh, "Real-time abdominal fetal ECG recording using a hardware correlator," *Comput. Biol. Med.*, vol. 22, pp. 332–335, 1992.

[9] S. L. Horner, W. M. Holls, and P. B. Crilly, "A robust real time algorithm for enhancing non-invasive foetal electrocardiogram," *Digital Signal Process.*, vol. 5, pp. 184–194, 1995.

[10] E. S. G. Genevier, A. C. Deans, M. C. Carter, and P. J. Steer, "Separation of fetal and maternal ECG complexes from a mixed signal using an algorithm based on linear regression," *Med. Eng. Phys.*, vol. 17, pp. 514–522, 1995.

[11] V. Zarzoso and A. K. Nandi, "Noninvasive fetal electrocardiogram extraction: blind separation versus adaptive noise cancellation," *IEEE Trans. Biomed. Eng.*, vol. 48, no. 1, pp. 12–18, Jan. 2001.

[12] D. M. Mooney, L. J. Grooome, L. S. Bentz, and J. D. Wilson, "Computer algorithm for adaptive extraction of fetal cardiac electrical signal," in *Proc. 1995 ACM Symp. Appl. Comput.*, Nashville, TN, 1995, pp. 113–117.

[13] M. Richter, T. Schreiber, and D. T. Kaplan, "Fetal ECG extraction with nonlinear state space projections," *IEEE Trans. Biomed. Eng.*, vol. 45, no. 1, pp. 133–137, Jan. 1998.

[14] G. Camps, M. Martinez, and E. Soria, "Fetal ECG extraction using an FIR neural network," in *Proc. Comput. Cardiol. 2001*, Rotterdam, The Netherlands, pp. 249–252.

[15] A. Kam and A. Cohen, "Detection of fetal ECG with IIR adaptive filtering and genetic algorithms," in *Proc. IEEE Int. Conf. Acoust., Speech Signal Process.*, vol. 4, Phoenix, AZ, Mar.1999, pp. 2335–2338.

[16] A. K. Barros and A. Cichocki, "Extraction of specific signals with temporal structure," *Neural Comput.*, vol. 13, pp. 1995–2003, 2001.

[17] K. A. K. Azad, "Fetal QRS complex detection from abdominal ECG: A fuzzy approach," in *Proc. IEEE Nordic Signal Process. Symp.*, Kolmarden, Sweden, 2000, pp. 275–278.

[18] A. Al-Zaden and A. Al-Smadi, "Extraction of foetal ECG by combination of singular value decomposition and neuro-fuzzy inference system," *Phys. Med. Biol.*, vol. 51, pp. 137–143, 2006.

[19] A. K. Barros, "Extracting the fetal heart rate variability using a frequency tracking algorithm," *Neurocomputing*, vol. 49, pp. 279–288, 2002.

[20] K. Assaleh and H. Al-Nashash, "A novel technique for the extraction of fetal ECG using polynomial networks," *IEEE Trans. Biomed. Eng.*, vol. 52, no. 6, pp. 1148–1152, Jun. 2005.

[21] Z. L. Zhang and Z. Yi, "Extraction of a source signal whose kurtosis value lies in a specific range," *Neurocomputing*, vol. 69, pp. 900–904, 2006.

[22] M. I. Ibrahimy, F. Ahmed, M. A. Mohd Ali, and E. Zahedi, "Real-time signal processing for fetal heart rate monitoring," *IEEE Trans. Biomed. Eng.*, vol. 50, no. 2, pp. 258–262, Feb. 2003.

[23] F. Mochimaru, F. Fujimoto, and Y. Ishikawa, "Detecting the fetal electrocardiogram by wavelet theory-based methods," *Progress Biomed. Res.*, vol. 7, pp. 185–193, 2002.

[24] A. Khamene and S. Negahdaripour, "A new method for the extraction of fetal ECG from the composite abdominal signal," *IEEE Trans. Biomed. Eng.*, vol. 47, no. 4, pp. 507–516, Apr. 2000.

[25] E. C. Karvounis, C. Papaloukas, D. I. Fotiadis, and L. K. Michalis, "Fetal heart rate extraction from composite maternal ECG using complex continuous wavelet transform," in *Proc. Comput. Cardiol. 2004*, Chicago, IL, pp. 19–22.

[26] A. Cichocki and S. Amari, *Adaptive Blind Signal and Image Processing*. West Sussex, U.K.: Wiley, 2002.

[27] A. K. Nandi and V. Zarzoso, "Foetal ECG separation," in *Proc. Inst. Electr. Eng. Colloq. Use Model Based Digital Signal Process. Tech. Anal. Biomed. Signals*, London, U.K., 1997, pp. 8/1–8/6.

[28] L. De Lathauwer, B. De Moor, and J. Vandewalle, "Fetal electrocardiogram extraction by blind source subspace separation," *IEEE Trans. Biomed. Eng.*, vol. 47, no. 5, pp. 567–572, May 2000.

[29] P. P. Kanjilal, S. Palit, and G. Saha, "Fetal ECG extraction from single-channel maternal ECG using singular value decomposition," *IEEE Trans. Biomed. Eng.*, vol. 44, no. 1, pp. 51–59, 1997.

[30] D. Callaerts, B. De Moor, J. Vandewalle, W. Sansen, G Vantrappen, and J. Janssens, "Comparison of SVD methods to extract the foetal electrocardiogram from cutaneous electrode signals," *Med. Biol. Eng. Comput.*, vol. 28, pp. 217–224, 1990.

[31] F. S. Najafabadi, A. Zahedi, and M. A. M. Ali, "Fetal heart rate monitoring based on independent component analysis," *Comput. Biol. Med.*, vol. 36, pp. 241–252, 2006.

[32] A. Kam and A. Cohen, "Separation of twins fetal ECG by means of blind source separation (BSS)," in *Proc. IEEE 21st Conv. Electr. Electron. Eng.*, Tel-Aviv, Israel, 2000, pp. 342–345.

[33] T. P. Jung, S. Makeig, T. W. Lee, M. J. McKeown, G. Brown, A. J. Bell, and T. J. Sejnowski, "Independent component analysis of biomedical signals," in *Proc. 2nd Int. Workshop Ind. Compon. Anal. Blind Signal Separation*, Helsinki, Finland, 2000, pp. 633–644.

[34] V. Vigneron, A. Paraschiv-Ionescu, A. Azancor, O. Sibony, and C. Jutten, "Fetal electrocardiogram extraction based on non-stationary ICA and wavelet denoising," in *Proc. 7th Symp. Signal Process. Appl.*, Paris, France, 2003, pp. 69–72.

[35] P. Gao, E. C. Chang, and L. Wyse, "Blind Separation of fetal ECG from single mixture using SVD and ICA," in *Proc. Inf., Commun. Signal Process. 4th Pacific-Rim Conf. Multimeda (CICS-PCM 2003)*, Singapore, 2003, pp. 1418–1422.

[36] D. E. Marossero, D. Erdogmus, N. R. Euliano, J. C. Principe, and K. E. Hild, "Independent components analysis for fetal electrocardiogram extraction: A case for the data efficient mermaid algorithm," in *Proc. Neural Netw. Signal Process.*, Toulouse, France, 2003, pp. 399–408.

[37] M. G. Jafari and J. A. Chambers, "Fetal electrocardiogram extraction by sequential source separation in the wavelet domain," *IEEE Trans. Biomed. Eng.*, vol. 52, no. 3, pp. 390–400, Mar. 2005.

[38] B. Azzerboni, F. L. Foresta, N. Mammone, and F. C. Morabito, "A new approach based on wavelet-ICA algorithms for fetal electrocardiogram extraction," in *Proc. 13th Eur. Symp. Artif. Neural Netw.*, Bruges, Belgium, 2005, pp. 27–29.

[39] R. L. Allen and D. W. Mills, *Signal Analysis: Time Frequency, Scale, and Structure*. Piscataway, NJ: IEEE Press, 2004.

[40] S. Qian, *Introduction to Time–Frequency and Wavelet Transforms*. Upper Saddle River, NJ: Prentice-Hall, 2001.

[41] F. Auger, P. Flandrin, P. Concalves, and O. Lemoine. (1996, Jan.). *Time–frequency toolbox: For use with MATLAB.* [Online]. Available: http://tftb.nongnu.org/

[42] B. Boashash, *Time–Frequency Signal Analysis*. Melboune, Australia: Longman-Cheshire/Wiley, 1992.

[43] S. Abboud and A. Beker, "An improved detection algorithm in fetal electrocardiography," *J. Electrocardiol.*, vol. 22 (suppl), pp. 238–242, 1989.

[44] I. Provazník, "Wavelet analysis for signal detection—Application to experimental cardiology research," Ph.D. dissertation, Dept. Biomed. Eng., Univ. Technol., Brno, Czech Republic, 2001.

[45] Mathworks Company. Wavelet tutorial of MATLAB. [Online]. Available: http://www.mathworks.com/access/helpdesk/help/toolbox/wavelet/wavelet.html

[46] P. S. Addison, "Wavelet transforms and the ECG: A review," *Physiol. Meas.*, vol. 26, pp. R155–R199, 2005.
[47] V. Johneff, "Complex valued wavelet analysis for QRS detection in ECG signals," in *Proc. 23rd Leeds Annu. Statistical Res. Workshop*, Leeds, U.K., 2004, pp. 134–36.
[48] A. Teolis, *Computational Signal Processing With Wavelets*. Boston, MA: Birkhauser, 1998.

Evaggelos C. Karvounis (S'07) was born in Ioannina, Greece, in 1978. He received the Diploma degree in computer science from the University of Thessaloniki, Thessaloniki, Greece, in 2002. He is currently working toward the Ph.D. degree at the University of Ioannina, Ioannina.

His current research interests include biomedical engineering, decision support systems in healthcare, and biomedical applications.

Markos G. Tsipouras (S'07) was born in Athens, Greece, in 1977. He received the Diploma and M.Sc. degrees in computer science from the University of Ioannina, Ioannina, Greece, in 1999 and 2002, respectively. He is currently working toward the Ph.D. degree at the University of Ioannina.

His current research interests include biomedical engineering, decision support and medical expert systems, and biomedical applications.

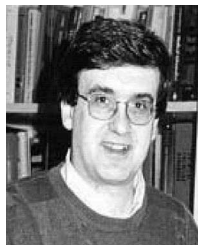

Dimitrios I. Fotiadis (M'01–SM'07) was born in Ioannina, Greece, in 1961. He received the Diploma degree in chemical engineering from National Technical University of Athens, Athens, Greece, in 1985 and the Ph.D. degree in chemical engineering from the University of Minnesota, Minneapolis, in 1990.

Since 1995, he has been with the Department of Computer Science, University of Ioannina, Ioannina, where he is currently an Associate Professor. He is the Director of the Unit of Medical Technology and Intelligent Information Systems. His current research interests include biomedical technology, biomechanics, scientific computing, and intelligent information systems.

Katerina K. Naka was born in Ioannina, Greece, in 1971. She received the Graduation degree with distinction from the Medical School, University of Ioannina, Ioannina, in 1994, and the Ph.D. degree from the University of Wales College of Medicine, Cardiff, Wales, U.K., in 2003.

She has completed her training in cardiology, and is currently a Lecturer of cardiology at the Medical School, University of Ioannina. Her current research interests include vascular endothelial function, large arterial mechanics, heart failure, and bioengineering.